JOURNAL OF MORPHOLOGY 273:1214–1226 (2012)

# Scaling of the Ballistic Tongue Apparatus in Chameleons

**Christopher V. Anderson,* Thomas Sheridan, and Stephen M. Deban**

*Department of Integrative Biology, University of South Florida, 4202 East Fowler Avenue SCA 110, Tampa, Florida 33620*

*ABSTRACT* Body dimensions of organisms can have a profound impact on their functional and structural properties. We examined the morphological proportions of the feeding apparatus of 105 chameleon specimens representing 23 species in seven genera, spanning a 1,000-fold range in body mass to test whether the feeding apparatus conforms to the null hypotheses of geometric similarity that is based on the prevalence of geometric similarity in other ectothermic vertebrates. We used a phylogenetically corrected regression analysis based on a composite phylogenetic hypothesis to determine the interspecific scaling patterns of the feeding apparatus. We also determined the intraspecific (ontogenetic) scaling patterns for the feeding apparatus in three species. We found that both intraspecifically and interspecifically, the musculoskeletal components of the feeding apparatus scale isometrically among themselves, independent of body length. The feeding apparatus is thus of conserved proportions regardless of overall body length. In contrast, we found that the tongue apparatus as a whole and its musculoskeletal components scale with negative allometry with respect to snout-vent length—smaller individuals have a proportionately larger feeding apparatus than larger individuals, both within and among species. Finally, the tongue apparatus as a whole scales with negative allometry with respect to body mass through ontogeny, but with isometry interspecifically. We suggest that the observed allometry may be maintained by natural selection because an enlarged feeding apparatus at small body size may maximize projection distance and the size of prey that smaller animals with higher mass-specific metabolic rates can capture. J. Morphol. 273:1214–1226, 2012. 

KEY WORDS: Chamaeleonidae; isometry; allometry; ontogeny; ballistic feeding

## INTRODUCTION

Body dimensions are known to have a considerable impact on a variety of functional and structural properties of organisms, perhaps most obviously in animal movement. Studies of locomotion have shown, for example, that small animals have higher absolute stride frequencies and accelerations than larger animals (Hill, 1950; Carrier, 1996). Changes in body size, however, are often accompanied by changes in shape (e.g., Carrier, 1996; Roos et al., 2010) confounding attempts to predict changes in movement performance based on body size alone.

Theoretical scaling models, which aim to predict how absolute dimensions will affect movement of musculoskeletal systems, are based on assumptions of similar relative dimensions of muscle and skeletal components (Hill, 1950; McMahon, 1973; McMahon and Bonner, 1983). Models based on this assumption of geometric similarity, or isometry (Hill, 1950; Richard and Wainwright, 1995) are frequently applied to feeding and locomotor systems (e.g., Choi et al., 2000; Toro et al., 2003; Deban and O'Reilly, 2005) but deviation from strict geometric similarity is common in a variety of systems (e.g., McMahon, 1973; Carrier, 1996; Birch, 1999; Erickson et al., 2003; Roos et al., 2010; Herrel et al., 2011).

Ectothermic vertebrates are an ideal system in which to test scaling models because closely related species often differ radically in body size and their individuals typically grow several orders of magnitude in body mass (O'Reilly, 1998; Meyers et al., 2002; Herrel et al., 2005). Scaling models predict that performance measures, such as velocity and acceleration, should scale with body length in a predictable way (e.g., Hill, 1950; McMahon, 1973; McMahon and Bonner, 1983; Richard and Wainwright, 1995). Hill (1950), for example, predicted that under geometric similarity velocity is size independent whereas acceleration declines are directly proportional to the increase in a characteristic length. Examining the morphological scaling patterns of organisms, as well as that of the musculoskeletal systems associated with given movements, is critical in any attempt to understand scaling patterns of performance.

Additional Supporting Information may be found in the online version of this article.

Contract grant sponsor: National Science Foundation; Contract grant number: IOS 0842626.

*Correspondence to: Christopher V. Anderson, Department of Integrative Biology, University of South Florida, 4202 East Fowler Avenue – SCA 110, Tampa, FL, 33620. E-mail: cvanders@mail.usf.edu

Received 22 July 2011; Revised 9 April 2012;
Accepted 23 May 2012

Published online 22 June 2012 in
Wiley Online Library (wileyonlinelibrary.com)
DOI: 10.1002/jmor.20053

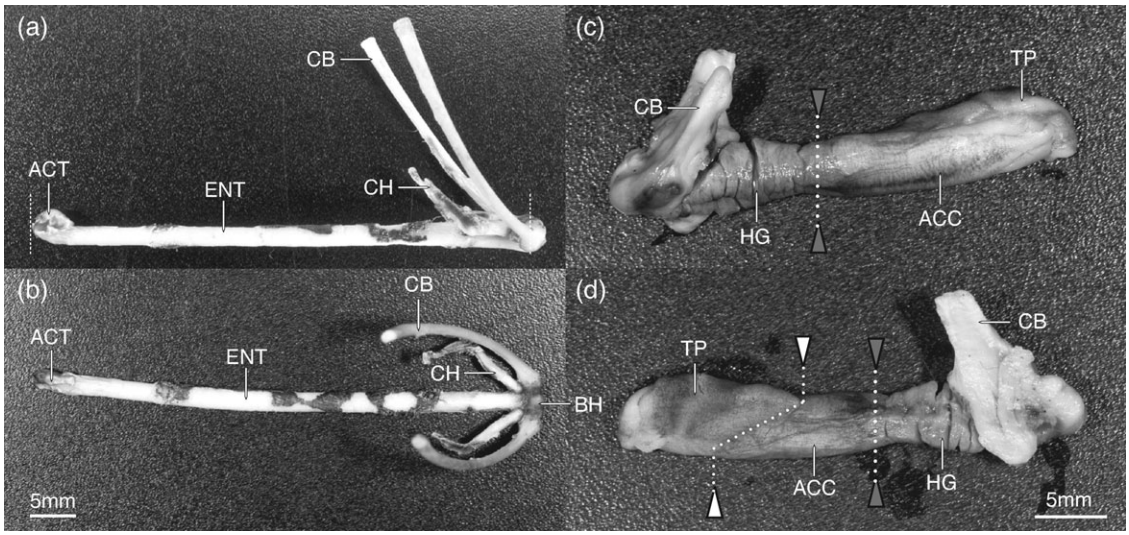


Fig. 1. Skeletal and muscular components of the chameleon tongue apparatus. Lateral (**a**) and dorsal (**b**) views of the skeletal elements of the chameleon tongue. Ventrolateral (**c**) and dorsolateral (**d**) views of the muscular elements of the chameleon tongue at rest. Anterior end of elements at left in (a), (b), and (d), and at right in (c). Scale bar at bottom left of figure associated with (a) and (b), and scale bar at bottom right of figure associated with (c) and (d). ACC, m. accelerator linguae; ACT, articulating cartilagenous tip; BH, basihyoid; CB, ceratobranchial; CH, ceratohyal; ENT, entoglossal process; HG, m. hyoglossus; TP, tongue pad. Dotted line in (a) indicate length of ENT as measured for analysis. Dotted lines between gray triangles in (c) and (d) indicate division between HG and ACC. Dotted line between white triangles in (d) indicate posterior limits of the TP. Anterior to the left in (a), (b), and (d), and to the right in (c).

Numerous studies of scaling patterns of locomotion and feeding systems exist (e.g., Hill, 1950; McMahon, 1973; Carrier, 1996; Meyers et al., 2002; Deban and O'Reilly, 2005; Herrel et al., 2005; Roos et al., 2010) and those that have examined ballistic mechanisms, which differ from many other movements in their reliance on momentum, have tended to focus on jumping (e.g., Marsh, 1994; Choi et al., 2000; Wilson et al., 2000). Scaling patterns of the hindlimbs in studies of frog jumping have been variable with hindlimb length scaling with positive allometry (Wilson et al., 2000), negative allometry (Marsh, 1994), and isometry (Choi et al., 2000; Wilson et al., 2000) relative to body mass in different taxa and age classes. Scaling patterns of locomotor systems, however, are often predicted to deviate from the assumption of geometric similarity to maintain safety factors on bones that support body weight as an organism's body mass increases (McMahon, 1973; McMahon and Bonner, 1983). Therefore, scaling patterns of locomotor ballistic movements, such as frog jumping, may not be good predictors of scaling patterns in non-locomotor ballistic movements such as tongue projection in frogs, salamanders or chameleons, in which body mass is neither supported nor accelerated.

We examined the morphological scaling patterns of the chameleon tongue apparatus as a model of a non-locomotor ballistic system. The morphology of the chameleon hyobranchial apparatus is highly conserved among taxa and is described in detail elsewhere (e.g., Houston, 1828; Gnanamuthu, 1930; Bell, 1989; Schwenk, 2000; Herrel et al., 2001; de Groot and van Leeuwen, 2004), so a description of only the structures relevant to this study is presented here. The chameleon's tongue is supported by the hyobranchial apparatus (tongue and throat skeleton; Fig. 1; Bell, 1989), the elongate entoglossal process (ENT) of which lies medially in the ventral portion of gular region along a rostrocaudal axis. The ENT is parallel-sided with a tapered anterior (i.e., rostral) tip and acts as a rigid structure for the tongue projector muscle, the m. accelerator linguae, to act against (Herrel et al., 2001). A pair of ceratobranchials and ceratohyals articulate with the basihyoid at the caudal end of the ENT (Bell, 1989; Herrel et al., 2001). The ceratobranchials and ceratohyals serve as attachment sites for the primary muscles involved in supporting and moving the hyobranchial apparatus, as well as the origin of the paired tongue retractor, the m. hyoglossus (Houston, 1828; Bell, 1989; Wainwright and Bennett, 1992; Herrel et al., 2001). The m. hyoglossus originates on the ceratobranchials and inserts on the m. accelerator linguae (Houston, 1828; Herrel et al., 2001). The posterior two-thirds to three-quarters of the m. accelerator linguae is cylindrically shaped with a central lumen encompassing the ENT while at rest. This tubular portion of the m. accelerator linguae is responsible for producing the forces and conformational changes responsible for tongue projection (Bell, 1989; Wainwright and Bennett, 1992;

van Leeuwen, 1997; Herrel et al., 2001; de Groot and van Leeuwen, 2004). At the distal end of the tongue, immediately anterior to the m. accelerator linguae, is the tongue pad, which is responsible for prey prehension.

We examined morphological scaling patterns of these skeletal elements and muscles of the tongue apparatus, which produce tongue projection and retraction in chameleons, to test whether the feeding apparatus conforms to the null hypothesis of geometric similarity. We compared both intraspecific and interspecific scaling patterns to determine how ontogenetic and evolutionary scaling patterns might differ. Based on our results, we predict how the observed scaling patterns may affect functional aspects of ballistic tongue projection, and discuss potential selective pressures that may act on the feeding apparatus of chameleons to shape these scaling patterns.

## MATERIALS AND METHODS

### Specimens and Phylogenetic Relationships

A total of 105 frozen specimens from 23 species in seven of the 11 currently recognized genera within the family Chamaeleonidae were examined (Table 1). All specimens were obtained post mortem from commercial and private sources within the contiguous United States. Specimens were frozen in blocks of ice immediately after death to keep their tissue hydrated, and only specimens deceased from conditions that would not affect the size and condition of their tongue apparatus were used. Following completion of the study, all specimens were deposited in the private collection of CV Anderson.

To estimate the relationships among chameleon species for phylogenetically corrected analysis, 15 composite phylogenies of differing topologies and branch lengths were constructed by combining the results from several molecular studies (Fig. 2; Townsend and Larson, 2002; Tilbury et al., 2006; Mariaux et al., 2008; Tilbury and Tolley, 2009a; Townsend et al., 2009, 2011).

Composite phylogenies of seven different topologies with branch lengths set to unity (Garland et al., 2005) were constructed to test the effects of tree topology on scaling trends (Fig. 2). Variation in the genus-level topology of trees is considerable, with studies indicating genera diverging in different orders and in some cases, being diphyletic. We based the initial topology of our composite phylogenies on four phylogenies (Townsend and Larson, 2002; Tilbury and Tolley, 2009a; Townsend et al., 2009, 2011) because the phylogenetic hypotheses in the other studies either did not include specimens from all genera examined in our study (Raxworthy et al., 2002) or were insufficiently resolved for our purposes, with polytomies of more than four branches (Tilbury et al., 2006). Single composite phylogenies were constructed based on the genus-level topology of Townsend and Larson (2002) (Fig. 2d) and Townsend et al. (2011) (Fig. 2a). Because the phylogenetic hypothesis from Townsend et al. (2009) recovered *Chamaeleo* as diphyletic, two composite phylogenies were constructed based on this study to place the *Chamaeleo* species from our study in both positions (Fig. 2b,c). Finally, three composite phylogenies were constructed from Tilbury and Tolley (2009a) to account for each possible topology of a three-branch polytomy (Fig. 2e–g). Intrageneric topologies were constructed based on Townsend and Larson (2002), Tilbury et al. (2006), Mariaux et al. (2008), Tilbury and Tolley (2009a), and Townsend et al. (2009). We followed Matthee et al. (2004), Tilbury et al. (2006) and Tilbury and Tolley (2009a) in recognizing the generic ranks of *Rieppeleon*, *Kinyongia*, and *Trioceros*, respectively.

To examine the effect of phylogenetic branch lengths on scaling trends, eight additional phylogenies of the same topology but with differing branch lengths were constructed for analysis. The topology of these phylogenies was based on the previously described composite phylogeny that was constructed based on the genus-level tree of Townsend et al. (2011) (Fig. 2a). We used the topology of this phylogenetic hypothesis, because it was the only one that was both well resolved and had branch lengths that were time calibrated with error bars. An initial phylogeny was constructed with branch lengths for all genus-level nodes set to their mean lengths, as depicted in Townsend et al. (2011). For within-genus branch lengths of genera in our data set with more than one species, the distance with error bars (Townsend et al., 2001) (Fig. 2a) to a node where within-genus branching begins was deduced from the published phylogeny. Branch lengths between this node and terminal taxa were evenly spaced. The branch lengths of this initial composite phylogeny were then varied along the node error bars to create a total of eight phylogenies with different branch length patterns. The initial phylogeny was based on average divergence times for both genus-level nodes and intrageneric nodes (Fig. 2a).

Because Townsend et al. (2011) did not depict error bars around the divergence time for *Rhampholeon*, three phylogenies were based on remaining genus-level nodes being shifted as distantly from the *Rhampholeon* node as their error bars allowed (i.e., divergence time of ancestral nodes was increased and divergence time of derived nodes was decreased). These three phylogenies varied in intrageneric branch lengths with one having the average divergence times for the intrageneric nodes, a second having these nodes shifted as far ancestrally as allowed by their error bars, and a third having these nodes shifted as far toward the terminal taxa as allowed by their error bars. Three additional phylogenies were based on genus-level nodes shifted as far toward the *Rhampholeon* node as allowed by their error bars while still maintaining topology (i.e., divergence time of ancestral nodes was decreased and divergence time of derived nodes was increased) and intrageneric nodes shifted as described previously. Finally, due to the noticeably long branch length for *Rieppeleon* in some published phylogenies (Townsend and Larson, 2002; Townsend et al., 2009), a final phylogeny was created based on average divergence times for both genus-level nodes and nodes where intrageneric nodes begin branching, but with the *Rieppeleon* node diverging as early as allowed by its error bars.

### Morphological Variables

Specimens were thawed and dissected to obtain measurements of skeletal elements and muscles of the tongue apparatus involved in tongue projection and retraction. An incision was made along the ventral midline from the sternum to the symphysis of the lower jaw. To free the tongue apparatus from the rest of the body, connective tissue attaching the tongue apparatus to the body was removed, the sternohyoideus muscle was severed at the sternum, and the geniohyoideus muscle was severed at the dentary. The m. accelerator linguae was removed and the m. hyoglossus was cut from the ceratobranchials where the muscle originates and detached from the ENT. As measurements were made, the tongue pad was dissected from the m. accelerator linguae.

Seven internal and external measurements were taken from each individual. Lengths were measured using Mitutoyo electronic calipers (±0.1 mm). Masses were measured with a Virtual Measurement and Control Model UB-302A electronic balance (±0.001 g) or a Denver Instruments SI-234 (±0.0001 g). Body mass and snout-vent length (SVL) of each chameleon specimen were collected as measures of body size. Body mass was measured prior to dissection. SVL was measured as the distance between the cloaca and the distal tip of the jaw symphysis. Jaw length was collected as an indication of oral cavity size, measured as the distance between the jaw symphysis and the jaw joint. The length of the ENT, around which the m. accelerator linguae contracts to power tongue projection, was measured from the cartilaginous tip to the basihyoid. The mass of the m. hyoglossus, which powers tongue retraction, was measured as the mass of the excised mus-

*TABLE 1. Summary of morphological measurements*

| Species | *n* | Mean ± SEM SVL (mm) | Mean ± SEM mass (g) | Mean ± SEM Jaw length (mm) | Mean ± SEM ENT length (mm) | Mean ± SEM HG mass (g) | Mean ± SEM ACC and TP mass (g) | Mean ± SEM ACC mass (g) |
|---|---|---|---|---|---|---|---|---|
| *Bradypodion transvaalense* | 8 | 37.2 ± 7.8 | 3.4 ± 1.8 | 9.8 ± 1.6 | 11.1 ± 1.7 | 0.026 ± 0.017 | 0.055 ± 0.028 | 0.032 ± 0.016 |
| *Chamaeleo africanus* | 1 | 128.5 | 48.3 | 30.1 | 28.5 | 0.395 | 0.725 | 0.424 |
| *C. calyptratus* | 11 | 110.9 ± 11.0 | 47.7 ± 10.1 | 26.1 ± 2.5 | 29.0 ± 2.4 | 0.258 ± 0.055 | 0.742 ± 0.138 | 0.471 ± 0.091 |
| *C. dilepis* | 1 | 117.0 | 23.3 | 22.7 | 31.9 | 0.180 | 0.671 | 0.398 |
| *Furcifer lateralis* | 4 | 83.6 ± 7.0 | 15.2 ± 2.7 | 20.3 ± 1.5 | 22.3 ± 1.0 | 0.095 ± 0.013 | 0.214 ± 0.052 | 0.133 ± 0.033 |
| *F. oustaleti* | 1 | 106.8 | 21.3 | 27.7 | 32.8 | 0.221 | 0.591 | 0.338 |
| *F. pardalis* | 22 | 121.5 ± 7.8 | 52.3 ± 8.3 | 29.2 ± 1.9 | 31.7 ± 1.7 | 0.276 ± 0.046 | 0.920 ± 0.125 | 0.541 ± 0.075 |
| *Kinyongia matschiei* | 2 | 116.2 ± 12.6 | 36.0 ± 8.9 | 27.9 ± 1.6 | 29.4 ± 2.3 | 0.209 ± 0.041 | 0.768 ± 0.104 | 0.423 ± 0.047 |
| *K. multituberculata* | 4 | 95.8 ± 6.7 | 15.6 ± 3.4 | 20.2 ± 1.4 | 22.2 ± 1.6 | 0.059 ± 0.010 | 0.192 ± 0.038 | 0.112 ± 0.030 |
| *K. tenuis* | 1 | 60.4 | 3.6 | 14.8 | 17.1 | 0.024 | 0.106 | 0.078 |
| *K. uthmoelleri artytor* | 1 | 71.2 | 9.4 | 21.4 | 19.3 | 0.053 | 0.182 | 0.098 |
| *K. xenorhina* | 1 | 88.9 | 12.3 | 27.9 | 22.9 | 0.098 | 0.203 | 0.158 |
| *Rhampholeon spinosus* | 1 | 46.4 | 2.4 | 14.6 | 15.1 | 0.015 | 0.048 | 0.039 |
| *Rieppeleon brevicaudatus* | 6 | 49.4 ± 2.1 | 3.0 ± 0.3 | 12.5 ± 0.4 | 15.3 ± 0.4 | 0.034 ± 0.010 | 0.086 ± 0.008 | 0.056 ± 0.006 |
| *Trioceros cristatus* | 1 | 99.3 | 13.3 | 22.7 | 31.8 | 0.169 | 0.404 | 0.263 |
| *T. deremensis* | 1 | 90.2 | 28.3 | 25.5 | 39.2 | 0.448 | 0.680 | 0.416 |
| *T. hoehnelii* | 10 | 48.9 ± 7.0 | 4.8 ± 1.8 | 12.9 ± 1.6 | 16.0 ± 2.1 | 0.031 ± 0.013 | 0.058 ± 0.018 | 0.038 ± 0.011 |
| *T. jacksonii xantholophus* | 4 | 112.1 ± 5.6 | 46.8 ± 8.2 | 25.7 ± 1.1 | 29.8 ± 1.0 | 0.193 ± 0.049 | 0.466 ± 0.032 | 0.312 ± 0.033 |
| *T. johnstoni* | 16 | 102.0 ± 5.4 | 32.5 ± 3.8 | 22.8 ± 1.0 | 28.0 ± 1.2 | 0.184 ± 0.022 | 0.399 ± 0.036 | 0.246 ± 0.022 |
| *T. melleri* | 3 | 137.4 ± 45.9 | 83.7 ± 62.8 | 35.1 ± 12.1 | 40.3 ± 12.0 | 0.340 ± 0.192 | 1.432 ±0.977 | 0.976 ± 0.664 |
| *T. perreti* | 3 | 67.2 ± 0.8 | 7.3 ± 1.4 | 15.3 ± 0.1 | 19.7 ± 1.5 | 0.045 ± 0.007 | 0.118 ± 0.014 | 0.097 ± 0.010 |
| *T. q. quadricornis* | 1 | 41.3 | 2.1 | 13.5 | 16.5 | 0.024 | 0.046 | 0.032 |
| *T. sternfeldi* | 2 | 76.9 ± 3.3 | 14.5 ± 0.0 | 18.1 ± 0.1 | 20.7 ± 1.7 | 0.068 ± 0.012 | 0.097 ± 0.051 | 0.069 ± 0.027 |

ACC, m. accelerator linguae; ENT, entoglossal process; HG, m. hyoglossus; SVL, Snout-Vent Length; TP, tongue pad.

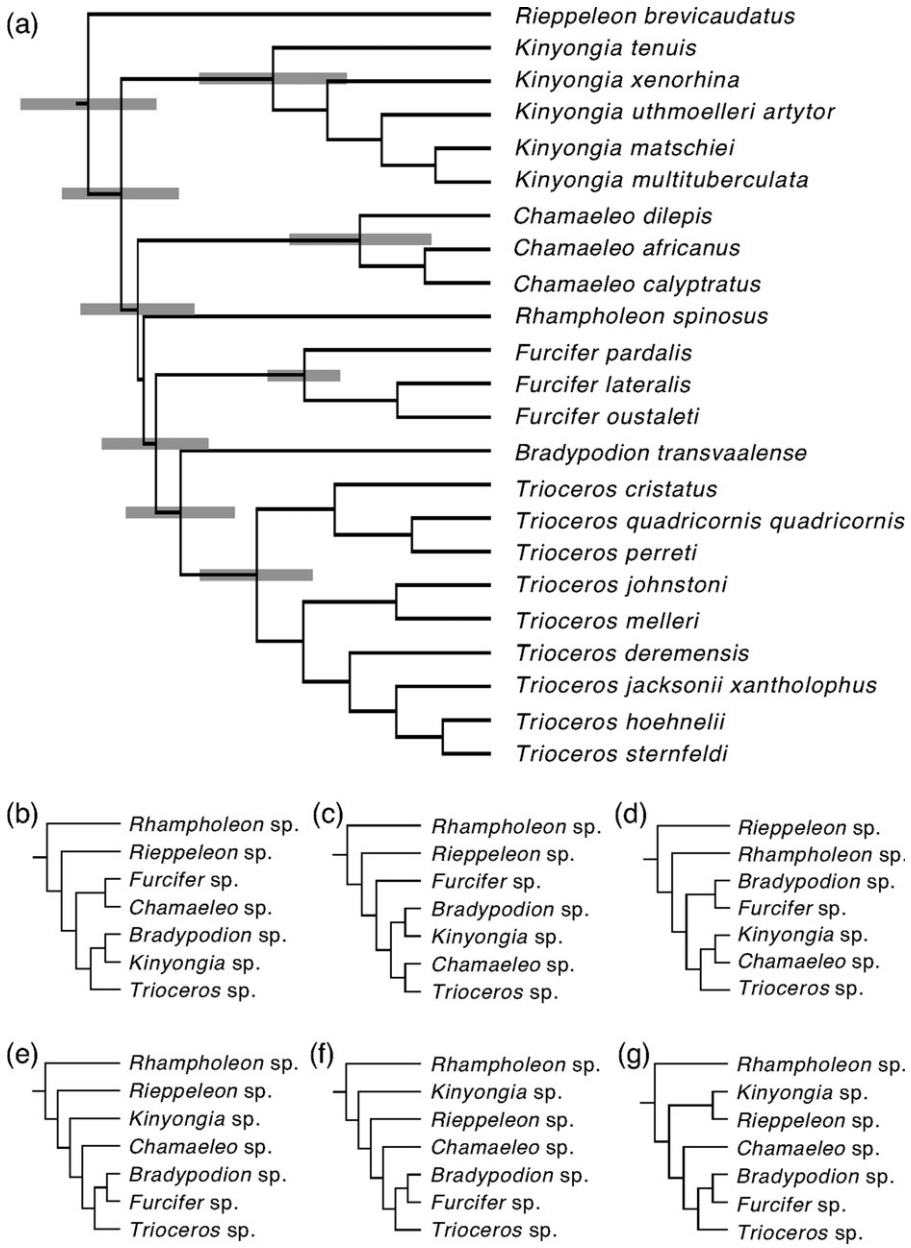


Fig. 2. Composite phylogenies estimating the relationships among species used in this study. Phylogenetic hypothesis based on genus-level topology and branch lengths with error bars (gray) of Townsend et al. (2011; **a**). Genus-level topologies based on Townsend and Larson (2002; **b**,**c**), Townsend et al. (2009; **d**), and Tilbury et al. (2009; **e**–**g**). Intrageneric topologies for analysis of (b–g) as in (a).

cle tissue between the base of the ENT and the junction between the m. hyoglossus and the m. accelerator linguae. The mass of the m. accelerator linguae and tongue pad, which, along with a portion of the m. hyoglossus, constitutes the total mass projected off the ENT, was measured as the mass of the tongue tissue with the m. hyoglossus removed. The mass of the m. accelerator linguae was measured after the tongue pad was removed.

## Expected Scaling Relationships

Expected scaling relationships between morphological characters were based on the predictions of isometry (geometric similarity) (Hill, 1950; McMahon and Bonner, 1983; Pennycuick, 1992). Under the predictions of isometry, morphological lengths are predicted to scale in direct proportion to each other (i.e., slope = 1.0), masses should scale as lengths to the power of 3 (i.e., slope = 3.0), and lengths are predicted to scale in proportion to mass to the 1/3 power (i.e., slope = 0.33).

## Interspecific Analysis

Prior to analysis, all measurements were log transformed. Log transforming morphological measurements allows scaling relationships between measurements to be examined using lin-

ear regression, in which the scaling relationship is the coefficient of the equation for the fitted line (i.e., slope). Regression coefficients from among-species contrasts were calculated using the Contrast program, PHYLIP, version 3.69 (Felsenstein, 2004) for each of the 15 composite phylogenies described above (Fig. 2). To account for within-species variation in the data, the W menu option of this program, which calculates contrasts based on both within- and among-species covariation, was used (Felsenstein, 2008). The output file produced from this analysis provides two sets of covariances, correlations and regressions. One set is for contrasts calculated based on only within-species phenotypic variation, while the second is for contrasts calculated based on both within- and among-species variation. To determine which method of contrast calculation is most appropriate, a likelihood ratio test for the absence of among-species variation is also produced. From the covariances, correlations and regressions given in the output files, 95% confidence limits of the regression coefficients were calculated based on the mathematical relationship between standard error of the regression coefficient and the output parameters (Bailey, 1995). These values were then compared to the expected slope based on an isometric scaling relationship (i.e., geometric similarity). Isometry was rejected for each scaling relationship if the expected regression coefficient did not fall within the 95% confidence limits of the observed regression coefficient.

### Intraspecific (Ontogenetic) Analysis

Data from three species for which we had more than 10 specimens varying significantly in SVL (*Furcifer pardalis*: 53.3–186.1 mm SVL, 3.9–147.9 g body mass; *Chamaeleo calyptratus*: 53.5–154.6 mm SVL, 3.9–90.6 g body mass; *Trioceros johnstoni*: 37.2–125.7mm SVL, 1.0–59.5g body mass; Table 1; Supporting Information Table S1) were used to examine intraspecific scaling patterns. Prior to analysis all measurements were log transformed.

Phylogenetic methods cannot be used in the absence of a hypothesis estimating relatedness among individuals, but accounting for relatedness of individuals of the same species is not necessary for our purposes. Therefore, we calculated intraspecific regression coefficients using a least-squares regression in Microsoft Excel 2004 for Mac OS X. As for the interspecific analysis, the regression coefficients of these relationships were then compared to their expected regression coefficients based on an isometric scaling relationship. Isometry was rejected for each scaling relationship if the expected regression coefficient fell outside the 95% confidence limits of the observed regression coefficient.

## RESULTS

### Interspecific Scaling Patterns

Specimens ranged in SVL from 20.8 to 223.0 mm (Table 1; Supporting Information S-Table 1), representing more than a 10-fold range in SVL, and ranged in total body mass from 0.2 to 208.2 g, representing more than a 1,000-fold range in body mass.

The likelihood ratio test for the absence of among-species phenotypic variation in the recorded anatomical measurements indicated for all phylogenetic hypotheses that among-species variation is present. Regression coefficients and their 95% confidence intervals were thus based on the among-species contrasts, which are affected by both within-species and among-species variation (as opposed to the within-species contrasts, which are affected only by within-species variation).

The seven phylogenetic topologies with branch lengths set to unity (Garland et al., 2005) used in this study exhibited minimal effects on scaling patterns (Table 2). Of 126 morphological scaling relationships examined across seven phylogenies, only two deviated from the scaling trend observed in the majority of phylogenies of different topology. Neither of these deviations in scaling relationships involved the same morphological measurements. In each of these cases, the observed trend is regarded as that seen in the majority of the phylogenies.

The eight phylogenetic hypotheses of the same topology but varying branch length exhibited a larger effect on scaling patterns than topological variation (Table 3). Of a total of 144 total morphological scaling relationships, eight deviated from the scaling trend observed in the majority of phylogenies of different branch lengths. Of these eight deviations in scaling relationships, six involved scaling patterns with respect to jaw length. As with the phylogenies of differing topologies, the observed trend for a given scaling relationship is regarded as that seen in the majority of phylogenies.

Comparing the observed scaling trends from the analysis of different topologies and the analysis of different branch lengths, four differences are noted. Among different topologies with branch lengths set to unity, contrast values for combined m. accelerator linguae and tongue pad mass relative to SVL scale with negative allometry (Table 2), while among different branch lengths of the same topology in a phylogenetic tree, contrast values for combined m. accelerator linguae and tongue pad mass relative to SVL scale with isometry (Table 3). Further, contrast values for m. hyoglossus mass, combined m. accelerator linguae and tongue pad mass, and m. accelerator linguae mass relative to jaw length all scale with isometry among phylogenies of different topologies with branch lengths set to unity (Table 2). Among trees of the same topology with different branch lengths, however, contrast values for hyoglossus mass, combined m. accelerator linguae and tongue pad mass, and m. accelerator linguae mass with respect to jaw length each scale with positive allometry in the majority of trees (Table 3).

Overall, a consistent pattern of negative allometry for contrast values of morphological variables relative to SVL was found for all variables, except for combined m. accelerator linguae and tongue pad mass (Tables 2 and 3; Figs. 3 and 4). Contrast values for jaw length relative to body mass scale with negative allometry, however, contrast values for all elements of the hyolingual apparatus relative to body mass scale with isometry (Tables 2 and 3; Fig. 4). Finally, contrast values for all hyolingual muscle masses relative to ENT length scale with isometry (Tables 2 and 3; Fig. 5).

*TABLE 2. Summary of interspecific regression coefficients to three significant figures from seven phylogenetic hypotheses with branch lengths set to unity*

| Function | Expected slope | Observed slope ± 95% confidence interval | | | | | | |
|---|---|---|---|---|---|---|---|---|
| | | Townsend et al., 2002 | Tilbury et al., 2009 - 1 | Tilbury et al., 2009 - 2 | Tilbury et al., 2009 - 3 | Townsend et al., 2009 - 1 | Townsend et al., 2009 - 2 | Townsend et al., 2011 |
| Jaw length vs. SVL | 1 | 0.83 ± 0.05[a] | 0.83 ± 0.05[a] | 0.84 ± 0.05[a] | 0.84 ± 0.05[a] | 0.82 ± 0.06[a] | 0.82 ± 0.05[a] | 0.81 ± 0.05[a] |
| ENT length vs. SVL | 1 | 0.87 ± 0.06[a] | 0.87 ± 0.06[a] | 0.87 ± 0.06[a] | 0.87 ± 0.06[a] | 0.88 ± 0.07[a] | 0.85 ± 0.07[a] | 0.88 ± 0.06[a] |
| Mass vs. SVL | 3 | 2.73 ± 0.08[a] | 2.70 ± 0.07[a] | 2.70 ± 0.07[a] | 2.71 ± 0.07[a] | 2.66 ± 0.09[a] | 2.69 ± 0.09[a] | 2.71 ± 0.07[a] |
| HG mass vs. SVL | 3 | 2.77 ± 0.18[a] | 2.72 ± 0.17[a] | 2.70 ± 0.16[a] | 2.71 ± 0.16[a] | 2.65 ± 0.19[a] | 2.62 ± 0.18[a] | 2.76 ± 0.17[a] |
| ACC and TP mass vs. SVL | 3 | 2.79 ± 0.17[a] | 2.74 ± 0.16[a] | 2.72 ± 0.15[a] | 2.73 ± 0.15[a] | 2.75 ± 0.18[a] | 2.75 ± 0.18[a] | 2.76 ± 0.16[a] |
| ACC mass vs. SVL | 3 | 2.75 ± 0.14[a] | 2.70 ± 0.14[a] | 2.68 ± 0.14[a] | 2.68 ± 0.13[a] | 2.72 ± 0.16[a] | 2.68 ± 0.15[a] | 2.70 ± 0.14[a] |
| Jaw length vs. mass | 0.333 | 0.302 ± 0.019[a] | 0.305 ± 0.018[a] | 0.308 ± 0.017[a] | 0.306 ± 0.017[a] | 0.304 ± 0.021[a] | 0.301 ± 0.019[a] | 0.296 ± 0.019[a] |
| ENT length vs. mass | 0.333 | 0.314 ± 0.023 | 0.317 ± 0.023 | 0.317 ± 0.023 | 0.316 ± 0.022 | 0.321 ± 0.027 | 0.310 ± 0.026 | 0.319 ± 0.023 |
| HG mass vs. mass | 1 | 1.01 ± 0.06 | 1.00 ± 0.06 | 1.00 ± 0.06 | 1.00 ± 0.06 | 0.99 ± 0.07 | 0.97 ± 0.07 | 1.02 ± 0.06 |
| ACC and TP mass vs. mass | 1 | 1.01 ± 0.06 | 1.00 ± 0.06 | 1.00 ± 0.06 | 1.00 ± 0.06 | 1.02 ± 0.07 | 1.01 ± 0.07 | 1.01 ± 0.06 |
| ACC mass vs. mass | 1 | 0.99 ± 0.05 | 1.00 ± 0.05 | 0.98 ± 0.05 | 0.98 ± 0.05 | 1.00 ± 0.07 | 0.98 ± 0.06 | 0.98 ± 0.05 |
| ENT length vs. jaw length | 1 | 1.01 ± 0.06 | 1.02 ± 0.06 | 1.02 ± 0.05 | 1.01 ± 0.06 | 1.03 ± 0.07 | 1.02 ± 0.06 | 1.05 ± 0.06 |
| HG mass vs. jaw length | 3 | 3.17 ± 0.20 | 3.16 ± 0.18 | 3.15 ± 0.16 | 3.14 ± 0.17 | 3.08 ± 0.21 | 3.08 ± 0.19 | 3.26 ± 0.19[a] |
| ACC and TP mass vs. jaw length | 3 | 3.12 ± 0.22 | 3.13 ± 0.20 | 3.12 ± 0.19 | 3.10 ± 0.20 | 3.12 ± 0.23 | 3.16 ± 0.22 | 3.20 ± 0.22 |
| ACC mass vs. jaw length | 3 | 3.09 ± 0.19 | 3.09 ± 0.17 | 3.07 ± 0.16 | 3.06 ± 0.17 | 3.09 ± 0.20 | 3.08 ± 0.19 | 3.14 ± 0.18 |
| HG mass vs. ENT length | 3 | 3.12 ± 0.08[a] | 3.07 ± 0.08 | 3.05 ± 0.08 | 3.06 ± 0.07 | 2.97 ± 0.09 | 3.01 ± 0.08 | 3.08 ± 0.08 |
| ACC AND TP mass VS. ENT length | 3 | 3.08 ± 0.12 | 3.04 ± 0.12 | 3.03 ± 0.11 | 3.04 ± 0.11 | 3.01 ± 0.13 | 3.10 ± 0.12 | 3.03 ± 0.12 |
| ACC mass vs. ENT length | 3 | 3.02 ± 0.11 | 2.98 ± 0.10 | 2.97 ± 0.10 | 2.97 ± 0.10 | 2.94 ± 0.12 | 3.00 ± 0.11 | 2.95 ± 0.10 |

Gray highlight indicates deviation from trend seen in remaining phylogenies.
Morphological abbreviations as in Table 1.
[a]Expected slope falls outside the 95% confidence interval around the observed slope indicating significant difference.

### Intraspecific (Ontogenetic) Scaling Patterns

Specimens of *C. calyptratus* (53.5–154.6 mm SVL; 3.9–90.6 g body mass), *F. pardalis* (53.3–186.1 mm SVL; 3.9–147.9 g body mass), and *T. johnstoni* (37.2–125.7 mm SVL; 1.0–59.5 g body mass) were used to examine intraspecific scaling patterns (Table 1; Supporting Information S-Table 1).

Relative to SVL, body mass scales with isometry for each species (Table 4), and jaw length and m. hyoglossus mass scale with isometry for two of the three species (Figs. 3 and 4). ENT length, combined m. accelerator linguae and tongue pad mass, and m. accelerator linguae mass, however, scale with negative allometry relative to SVL for each species (Fig. 4).

Relative to body mass (Table 4), ENT length, combined m. accelerator linguae and tongue pad mass, and m. accelerator linguae mass scale with negative allometry (Fig. 4). Jaw length and m. hyoglossus mass, conversely, scale with isometry relative to body mass for two of the three species.

Relative to jaw length (Table 4), m. accelerator linguae mass scales with negative allometry for each species while scaling patterns for all other hyolingual apparatus elements varied. M. hyoglossus mass and combined m. accelerator linguae and tongue pad mass both scaled with isometry relative to jaw length in two of the three species, whereas ENT length scaled with negative allometry in two of the three species.

Finally, all hyolingual muscle masses tended to scale with isometry relative to ENT length (Table 4; Fig. 5). In *T. johnstoni*, however, m. accelerator linguae mass scaled with negative allometry relative to ENT length.

## DISCUSSION

Scaling patterns showing geometric similarity ontogenetically and interspecifically are prevalent in ectothermic vertebrates. For example, the nurse shark, *Ginglymostoma cirratum*, exhibits isometric growth of the feeding apparatus relative to both head and total length (Robinson and Motta, 2002) and the largemouth bass, *Micropterus salmoides*, exhibits geometric similarity of the muscles and lever arms of the lower jaw relative to standard length (Richard and Wainwright, 1995). Both ontogenetically and interspecifically, limb dimensions of *Anolis* lizards tend to exhibit isometric growth relative to SVL (Toro et al., 2003). Similarly, among two species of spiny lizards (*Sceloporus*) and among two species of whiptail lizards (*Aspidoscelis*) head width and head height scale isometrically relative to SVL (Meyers et al., 2002). Finally, among 28 turtle species carapace width, body mass, and cranial dimensions scale with geometric similarity relative to carapace length (Herrel et al., 2002). Based on the prevalence of geometric

*TABLE 3. Summary of interspecific regression coefficients to three significant figures from phylogenetic hypothesis based on Townsend et al. (2011) with varying branch lengths*

| | | Observed slope ± 95% confidence interval | | | | | | | |
|---|---|---|---|---|---|---|---|---|---|
| Function | Expected slope | Average | Away/ Ancestral | Away/ Average | Away/ Terminal | Toward/ Ancestral | Toward/ Average | Toward/ Terminal | Early *Rieppeleon*/ Average |
| Jaw length vs. SVL | 1 | 0.82 ± 0.05[a] | 0.83 ± 0.05[a] | 0.82 ± 0.05[a] | 0.81 ± 0.05[a] | 0.82 ± 0.05[a] | 0.81 ± 0.05[a] | 0.80± 0.05[a] | 0.81 ± 0.05[a] |
| ENT length vs. SVL | 1 | 0.89 ± 0.06[a] | 0.89 ± 0.06[a] | 0.87 ± 0.06[a] | 0.88 ± 0.08[a] | 0.87 ± 0.06[a] | 0.86 ± 0.07[a] | 0.86 ± 0.07[a] | 0.87 ± 0.07[a] |
| Mass vs. SVL | 3 | 2.71 ± 0.06[a] | 2.73 ± 0.07[a] | 2.73 ± 0.07[a] | 2.70 ± 0.06[a] | 2.73 ± 0.07[a] | 2.71 ± 0.07[a] | 2.69 ± 0.06[a] | 2.71 ± 0.06[a] |
| HG mass vs. SVL | 3 | 2.75 ± 0.16[a] | 2.77 ± 0.16[a] | 2.71 ± 0.16[a] | 2.74 ± 0.16[a] | 2.71 ± 0.16[a] | 2.70 ± 0.16[a] | 2.70 ± 0.16[a] | 2.72 ± 0.16[a] |
| ACC and TP mass vs. SVL | 3 | 2.88 ± 0.16 | 2.87 ± 0.16 | 2.84 ± 0.17 | 2.92 ± 0.17 | 2.84 ± 0.17 | 2.87 ± 0.17 | 2.91 ± 0.18 | 2.88 ± 0.17 |
| ACC mass vs. SVL | 3 | 2.79 ± 0.14[a] | 2.79 ± 0.14[a] | 2.75 ± 0.15[a] | 2.82 ± 0.15[a] | 2.75 ± 0.15[a] | 2.77 ± 0.15[a] | 2.80 ± 0.16[a] | 2.79 ± 0.15[a] |
| Jaw length vs. mass | 0.333 | 0.295 ± 0.020[a] | 0.297 ± 0.020[a] | 0.293 ± 0.020[a] | 0.292 ± 0.021[a] | 0.294 ± 0.020[a] | 0.292 ± 0.021[a] | 0.289 ± 0.022[a] | 0.291 ± 0.021[a] |
| ENT length vs. mass | 0.333 | 0.317 ± 0.027 | 0.318 ± 0.026 | 0.309 ± 0.026 | 0.316 ± 0.029 | 0.310 ± 0.026 | 0.309 ± 0.028 | 0.309 ± 0.039 | 0.312 ± 0.028 |
| HG mass vs. mass | 1 | 1.00 ± 0.06 | 1.00 ± 0.06 | 0.98 ± 0.06 | 0.99 ± 0.07 | 0.98 ± 0.06 | 0.98 ± 0.06 | 0.98 ± 0.07 | 0.99 ± 0.06 |
| ACC and TP mass vs. mass | 1 | 1.03 ± 0.07 | 1.03 ± 0.07 | 1.01 ± 0.07 | 1.05 ± 0.08 | 1.01 ± 0.07 | 1.02 ± 0.08 | 1.04 ± 0.08 | 1.03 ± 0.08 |
| ACC mass vs. mass | 1 | 1.00 ± 0.07 | 1.00 ± 0.06 | 0.98 ± 0.07 | 1.01 ± 0.07 | 0.98 ± 0.07 | 0.99 ± 0.07 | 1.01 ± 0.08 | 1.00 ± 0.07 |
| ENT length vs. jaw length | 1 | 1.06 ± 0.06 | 1.05 ± 0.06 | 1.03 ± 0.06 | 1.08 ± 0.06[a] | 1.03 ± 0.06 | 1.04 ± 0.06 | 1.06 ± 0.06 | 1.06 ± 0.06 |
| HG mass vs. jaw length | 3 | 3.22 ± 0.18[a] | 3.21 ± 0.18[a] | 3.16 ± 0.19 | 3.25 ± 0.19[a] | 3.16 ± 0.19 | 3.18 ± 0.19 | 3.21 ± 0.19[a] | 3.22 ± 0.19[a] |
| ACC and TP mass vs. jaw length | 3 | 3.33 ± 0.22[a] | 3.29 ± 0.21[a] | 3.28 ± 0.22[a] | 3.42 ± 0.23[a] | 3.27 ± 0.22[a] | 3.33 ± 0.23[a] | 3.43 ± 0.24[a] | 3.26 ± 0.22[a] |
| ACC mass vs. jaw length | 3 | 3.24 ± 0.19[a] | 3.21 ± 0.18[a] | 3.18 ± 0.19 | 3.32 ± 0.20[a] | 3.17 ± 0.19 | 3.22 ± 0.20[a] | 3.31 ± 0.21[a] | 3.27 ± 0.19[a] |
| HG mass vs. ENT length | 3 | 3.00 ± 0.08 | 3.01 ± 0.09 | 3.02 ± 0.09 | 2.98 ± 0.08 | 3.02 ± 0.09 | 3.01 ± 0.09 | 2.99 ± 0.09 | 3.01 ± 0.08 |
| ACC and TP mass vs. ENT length | 3 | 3.09 ± 0.14 | 3.07 ± 0.14 | 3.12 ± 0.14 | 3.14 ± 0.14 | 3.12 ± 0.14 | 3.15 ± 0.14[a] | 3.20 ± 0.14[a] | 3.13 ± 0.14 |
| ACC mass vs. ENT length | 3 | 3.00 ± 0.11 | 2.98 ± 0.11 | 3.01 ± 0.12 | 3.03 ± 0.11 | 3.01 ± 0.12 | 3.04 ± 0.12 | 3.07 ± 0.12 | 3.03 ± 0.11 |

Observed slope subcolumn names indicate how branch lengths were established. Term prior to slash refers to genus-level nodes while term following slash refers to initial node of within-genus divergence. "Average" indicates nodes were set to the average divergence. "Away" indicates that genus level nodes were shifted as distantly away from the *Rhampholeon* node as allowed by their error bars while "Toward indicates these nodes were shifted as closely toward the *Rhampholeon* node as possible while still maintaining topology. "Ancestral" indicates that within-genus divergence nodes were shifted as ancestrally as allowed by their error bars while "Terminal" indicates these nodes were shifted as far toward the terminal taxa as allowed by their error bars. Gray highlight indicates deviation from trend seen in remaining phylogenies. Morphological abbreviations as in Table 1.

[a]Expected slope falls outside the 95% confidence interval around the observed slope indicating significant difference.

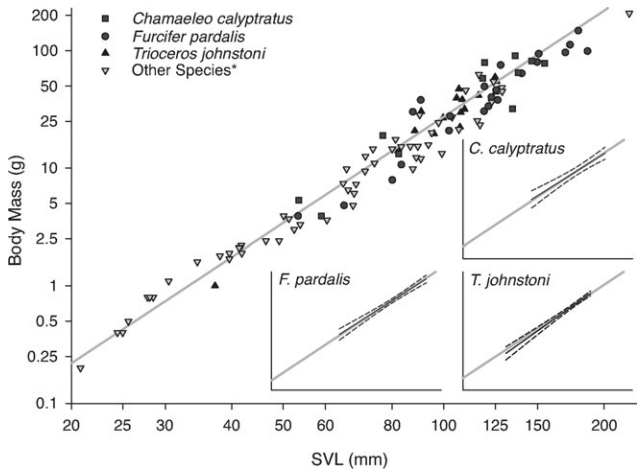


Fig. 3. Scaling relationships with respect to SVL for body mass. Solid gray lines represent isometric slope. Primary graph depicts raw data for all species with respect to line of isometric slope and inset graphs depict intraspecific (ontogenetic) scaling relationships for the species noted at the top left of each inset graph. Raw data are depicted in primary graph because the interspecific analysis program PHYLIP does not output independent contrasts. Shapes correspond to individual data points of different taxa. Dark gray lines in inset graphs represent scaling relationships (i.e., least squares regression) of different taxa with 95% confidence intervals around each relationship represented by colored dashed lines. Squares represent data for *C. calyptratus*. Circles represent data for *F. pardalis*. Triangles represent data for *T. johnstoni*. Hollow upside-down triangles represent data for all remaining specimens of other species. Inset graphs cover same range of values on *x*- and *y*-axes as primary graph. Isometric slope falling outside the 95% confidence interval around the observed slope for a given taxon (i.e., significant difference) for each relationship is indicated by * following the taxon name in the legend of primary graph. Significant difference between isometric slope and observed interspecific scaling relationship of all individuals for each relationship is indicated by * following "Other Species" label in key.

similarity in other ectothermic vertebrates, chameleons may be expected to scale geometrically in their morphological dimensions, both through ontogeny and among-species.

Our data indicate that the muscular and skeletal components of the tongue apparatus are conserved in relative proportions (Tables 2–4; Fig. 5) as predicted from the patterns observed in other ectothermic vertebrates. In contrast, the apparatus as a whole is proportionately larger in chameleons of shorter body length, both through ontogeny (Table 4; Fig. 4) and among species (Tables 2 and 3; Fig. 4), diverging from the pattern observed in other ectothermic vertebrates. The general scaling pattern of the tongue apparatus relative to body mass also differs between interspecific and ontogenetic comparisons (Tables 2–4; Fig. 4).

Based on the proportionately larger tongue apparatus in smaller chameleons, a few predictions of tongue projection performance can be made. Geometric similarity predicts that average velocity is independent of body size and that as size increases, acceleration decreases (Hill, 1950). In fact, because acceleration is proportional to velocity change over time and time during movement is proportional to length (Pennycuick, 1992), acceleration should change at a rate inversely proportional to the change in length. Further, because mechanical power output scales with the two-thirds power of mass (Pennycuick, 1992), mass-specific power output would scale inversely with the one-third power of mass, which is equivalent to scaling proportionately to the inverse of length. Consequently, we would expect a smaller tongue apparatus to project its tongue at a similar velocity but higher acceleration and mass-specific power than a larger apparatus. This prediction is consistent with scaling of performance in another ballistic system, jumping in post-metamorphic striped marsh frogs, *Limnodynastes peronii*, in which both total jumping distance and take-off velocity were found to be mass-independent over a body mass range of 2.9–38.4 g, while maximum jumping acceleration declined as mass increased. Because the chameleon tongue apparatus scales with negative allometry relative to SVL, however, accelerations and mass-specific power outputs should be disproportionately lower in smaller chameleons than predicted from the assumption of geometric similarity. Finally, because m. hyoglossus mass scales with negative allometry relative to SVL among different species (Tables 2 and 3; Fig. 4), we expect smaller species to have proportionately larger, and thus longer, m. hyoglossus than larger species, thus explaining their proportionately longer maximum tongue projection distances (Anderson, personal observation).

Numerous selective pressures may be acting on the feeding apparatus of chameleons to shape the scaling patterns we observe. First, the negative allometry of the feeding apparatus, as a whole, relative to SVL, combined with the conserved relative proportions within the feeding mechanism, itself, is not unexpected. Selection on performance in juvenile life-history stages is suggested to result in allometric scaling patterns during ontogeny that raise juvenile performance to levels comparable to those of adults (Carrier, 1996; Roos et al., 2010; Herrel et al., 2011). Juvenile seahorses, *Hippocampus reidi*, for example, have snout proportions that scale allometrically during ontogeny, and as a consequence juveniles were predicted to exhibit performance levels close to those of adults (Roos et al, 2010). Further, in the viper *Cryptelytrops albolabris*, head dimensions and head mass scale with negative allometry to body mass, and strike velocity and distance is independent of body size (Herrel et al., 2011). In chameleons, as tongue size increases, so too should the size of prey items a chameleon is able to capture due to an increase in the size of the tongue pad. By having a disproportionately large feeding apparatus, juvenile chameleons might increase their competitive advantage

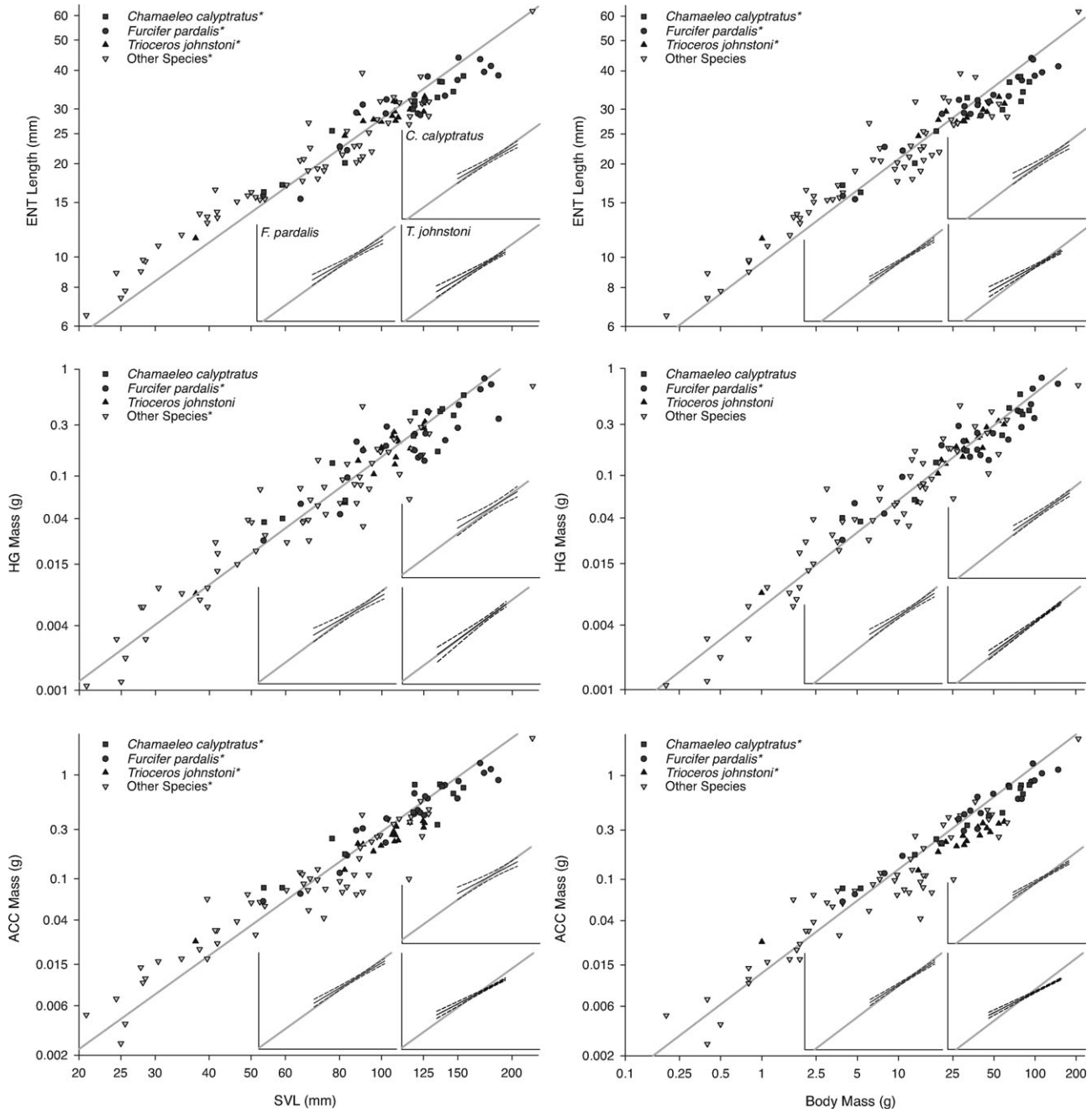


Fig. 4. Scaling relationships for ENT length, m. hyoglossus (HG) mass, and m. accelerator linguae (ACC) mass with respect to SVL (left) and ENT length (right). Indications as in Fig. 3. Species affiliated with inset graphs are the same layout for each primary graph as in top left primary graph.

over conspecifics and other competitors by broadening their resource base (Meyers et al., 2002).

The ability to capture prey of larger sizes due to a proportionately larger tongue apparatus in young individuals may have metabolic advantages as well. Because mass-specific metabolic rates are higher in small animals (Templeton, 1970; Whitford, 1973; Hayssen and Lacy, 1985; McKechnie and Wolf, 2004), including chameleons (Zari, 1993), the ability to take advantage of larger energy-rich prey items may be particularly beneficial for young chameleons (Meyers et al., 2002). Although metabolic rates and the growth of traits driven by metabolic demands are predicted to scale relative to body mass raised to a power of 0.67 or 0.75 (Kleiber, 1932; McMahon and Bonner, 1983), measurements of metabolic rate scaling have been found to be variable. For example, metabolic rates of scleroglossan

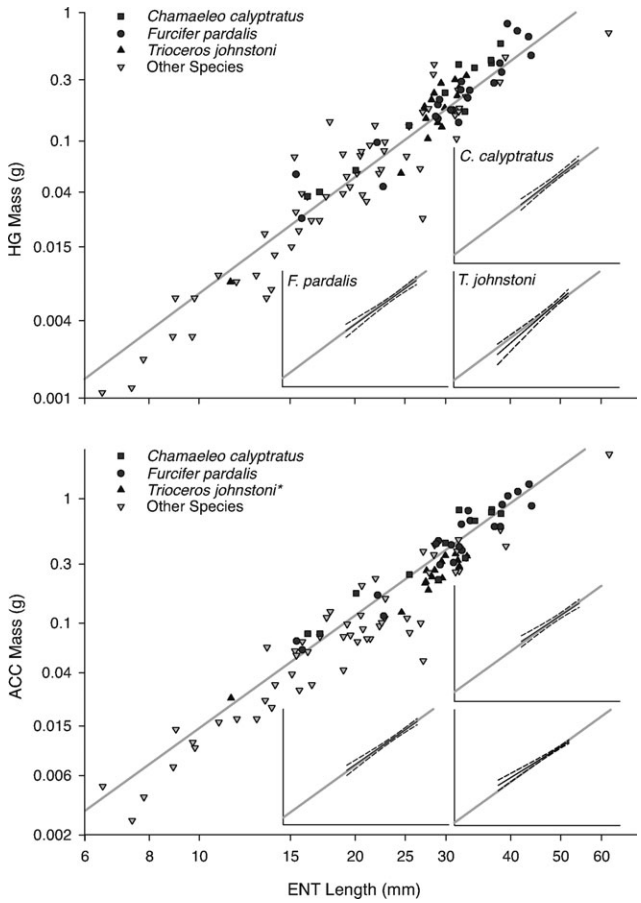


Fig. 5. Scaling relationships for m. hyoglossus (HG) mass, and m. accelerator linguae (ACC) mass with respect to ENT length. Indications as in Fig. 3. Species affiliated with inset graphs are the same layout for each primary graph as in top left primary graph.

lizards scale with a power of 0.95 with respect to body mass, whereas Iguanian lizards scale with a power of 0.79 (Nagy et al., 1999). Through ontogeny, the chameleon feeding apparatus and its components scale with negative allometry relative to body mass and fall within the general scaling range of 0.66–0.92, the range either measured or predicted for metabolism-driven scaling (Table 4; Fig. 4; Kleiber, 1932; McMahon and Bonner, 1983; Nagy et al., 1999). During ontogeny, when growth rates are determined by energy input, scaling of metabolic rates may be one factor influencing the observed negatively allometric scaling trend of the feeding apparatus relative to body mass.

Small chameleons may additionally be under selection pressure to minimize certain performance parameters, such as accelerations, and maximize others, such as the size of the projectile portion of the tongue, to reduce energy loss during tongue projection. Tongue projection in chameleons is characterized by high accelerations—exceeding 41 *g* in adult *C. calyptratus* (Anderson and Deban, 2010). Accelerations in musculoskeletal systems generally increase with decreasing dimensions (Hill, 1950; Pennycuick, 1992), so a smaller tongue apparatus is expected to exhibit higher accelerations. High accelerations, however, may be unfavorable when projecting soft tissues because internal deformations can result in energy loss (Müller and Kranenbarg, 2004). Further, projectiles of small size lose a higher proportion of energy to air resistance than projectiles of larger size and thus travel shorter distances (McMahon and Bonner, 1983). Small chameleons, both interspecifically and ontogenetically, may thus reduce energy loss during tongue projection and increase tongue

*TABLE 4. Summary of intraspecific regression coefficients to three significant figures*

| Function | Expected slope | Observed slope ± 95% confidence interval | | |
|---|---|---|---|---|
| | | *Chamaeleo calyptratus* | *Furcifer pardalis* | *Trioceros johnstoni* |
| Jaw length vs. SVL | 1 | 0.88 ± 0.26 | 0.93 ± 0.12 | 0.80 ± 0.12[a] |
| ENT length vs. SVL | 1 | 0.80 ± 0.15[a] | 0.79 ± 0.16[a] | 0.80 ± 0.14[a] |
| Mass vs. SVL | 3 | 2.86 ± 0.74 | 2.90 ± 0.44 | 3.22 ± 0.42 |
| HG mass vs. SVL | 3 | 2.47 ± 0.71 | 2.34 ± 0.58[a] | 2.97 ± 0.52 |
| ACC and TP mass vs. SVL | 3 | 2.26 ± 0.66[a] | 2.48 ± 0.32[a] | 2.28 ± 0.35[a] |
| ACC mass vs. SVL | 3 | 2.21 ± 0.62[a] | 2.49 ± 0.34[a] | 2.18 ± 0.26[a] |
| Jaw length vs. mass | 0.333 | 0.295 ± 0.074 | 0.305 ± 0.040 | 0.244 ± 0.030[a] |
| ENT length vs. mass | 0.333 | 0.263 ± 0.059[a] | 0.273 ± 0.034[a] | 0.246 ± 0.037[a] |
| HG mass vs. mass | 1 | 0.85 ± 0.15 | 0.81 ± 0.15[a] | 0.92 ± 0.10 |
| ACC and TP mass vs. mass | 1 | 0.80 ± 0.06[a] | 0.82 ± 0.10[a] | 0.71 ± 0.06[a] |
| ACC mass vs. mass | 1 | 0.77 ± 0.09[a] | 0.83 ± 0.09[a] | 0.66 ± 0.06[a] |
| ENT length vs. jaw length | 1 | 0.82 ± 0.25 | 0.85 ± 0.13[a] | 0.71 ± 0.22[a] |
| HG mass vs. jaw length | 3 | 2.61 ± 0.78 | 2.56 ± 0.46 | 3.63 ± 0.58[a] |
| ACC and TP mass vs. jaw length | 3 | 2.47 ± 0.57 | 2.54 ± 0.37[a] | 2.82 ± 0.29 |
| ACC mass vs. jaw length | 3 | 2.40 ± 0.53[a] | 2.58 ± 0.35[a] | 2.65 ± 0.31[a] |
| HG mass vs. ENT length | 3 | 3.10 ± 0.54 | 2.86 ± 0.53 | 3.50 ± 0.68 |
| ACC and TP mass vs. ENT length | 3 | 2.81 ± 0.62 | 2.86 ± 0.41 | 2.77 ± 0.28 |
| ACC mass vs. ENT length | 3 | 2.73 ± 0.56 | 2.87 ± 0.42 | 2.57 ± 0.36[a] |

Morphological abbreviations as in Table 1. Gray highlight indicates deviation from trens seen in remaining species.
[a]Expected slope falls outside the 95% confidence interval around the observed slope indicating significant difference.

projectile range by possessing a proportionately larger, and thus heavier, tongue apparatus (Tables 2–4; Fig. 4) that produces lower accelerations during launch.

Finally, the interspecific pattern of body mass scaling with negative allometry relative to SVL, and thus, the tongue apparatus scaling with negative allometry relative to SVL but with isometry relative to body mass, could be related to the arboreality of chameleons and the relationship between body length and body mass (Tables 2 and 3; Fig. 3). To distribute their weight over a larger area, arboreal snakes, for example, are longer and thinner than terrestrial species (Martins et al., 2001; Pizzatto et al., 2007). Similarly chameleons are proportionately longer for their body mass compared to other lizards, which distributes their mass over a larger area, potentially expanding the spatial niche of larger species by enabling them to use additional, smaller, branch diameters.

## ACKNOWLEDGMENTS

The authors thank M. Lajeunesse and J. Rohr for helpful consultation during the analysis of data for this manuscript, S. Creemers, N. Larghi, J. Richardson and J. Zona for helpful suggestions on drafts of this manuscript and D. Carver, E. Hinkle, N. Mole, M. Monge and P. Reid for assistance in specimen acquisition.

## LITERATURE CITED

Anderson CV, Deban SM. 2010. Ballistic tongue projection in chameleons maintains high performance at low temperature. Proc Natl Acad Sci USA 107:5495–5499.

Bailey NTJ. 1995. Statistical Methods in Biology. Third Edition. Cambridge: Cambridge University Press.

Bell DA. 1989. Functional anatomy of the chameleon tongue. Zool Jb Anat 119:313–336.

Birch JM. 1999. Skull allometry in the marine toad, *Bufo marinus*. J Morphol 241:115–126.

Carrier DR. 1996. Ontogenetic limits on locomotor performance. Physiol Zool 69:467–488.

Choi IH, Shim JH, Lee YS, Ricklefs RE. 2000. Scaling of jumping performance in anuran amphibians. J Herpetol 34: 222–227.

de Groot JH, van Leeuwen JL. 2004. Evidence for an elastic projection mechanism in the chameleon tongue. Proc R Soc B 271:761–770.

Deban SM, O'Reilly JC. 2005. The ontogeny of feeding kinematics in a giant salamander *Cryptobranchus alleganiensis*: Does current function or phylogenetic relatedness predict the scaling patterns of movement? Zoology 108:155–167.

Erickson GM, Lappin AK, Vliet KA. 2003. The ontogeny of bite-force performance in American alligator (*Alligator mississippiensis*). J Zool Lond 260:317–327.

Felsenstein J. 2004. PHYLIP (Phylogeny Inference Package) version 3.69. Distributed by the author. Seattle: Department of Genome Sciences, University of Washington.

Felsenstein J. 2008. Comparative methods with sampling error and within-species variation: Contrasts revisited and revised. Am Nat 171:713–725.

Garland T, Bennett AF, Rezende EL. 2005. Phylogenetic approaches in comparative physiology. J Exp Biol 208:3015–3035.

Gnanamuthu CP. 1930. The anatomy and mechanism of the tongue of *Cham?leon carcaratus* (Merrem). Proc Zool Soc Lond 31:467–486.

Hayssen V, Lacy RC. 1985. Basal metabolic rates in mammals: Taxonomic differences in the allometry of BMR and body mass. Comp Biochem Physiol A 81:741–754.

Herrel A, Huyghe K, Okovic P, Lisicic D, Tadic Z. 2011. Fast and furious: effects of body size on strike performance in an aboreal viper *Trimeresurus (Cryptelytrops) albolabris*. J Exp Zool 315A:22–29.

Herrel A, Meyers JJ, Nishikawa KC, De Vree F. 2001. Morphology and histochemistry of the hyolingual apparatus in chameleons. J Morphol 249:154–170.

Herrel A, O'Reilly JC, Richmond AM. 2002. Evolution of bite performance in turtles. J Evol Biol 15:1083–1094.

Herrel A, Van Wassenbergh S, Wouters S, Adriaens D, Aerts P. 2005. A functional morphological approach to the scaling of the feeding system in the African catfish, *Clarias gariepinus*. J Exp Biol 208:2091–2102.

Hill AV. 1950. The dimensions of animals and their muscular dynamics. Sci Prog 38:209–230.

Houston J. 1828. On the structure and mechanism of the tongue of the chameleon. Trans R Irish Acad 15:177–201.

Kleiber M. 1932. Body size and metabolism. Hilgardia 6:315–353.

Mariaux J, Lutzmann N, Stipala J. 2008. The two-horned chameleons of East Africa. Zool J Linn Soc 152:367–391.

Marsh RL. 1994. Jumping ability of anuran amphibians. Adv Vet Sci Comp Med 38B:51–111.

Martins M, Araujo MS, Sawaya RJ, Nunes R. 2001. Diversity and evolution of macrohabitat use, body size and morphology in a monophyletic group of Neotropical pitvipers (*Bothrops*). J Zool, Lond 254:529–538.

Matthee CA, Tilbury CR, Townsend T. 2004. A phylogenetic review of the African leaf chameleons: genus *Rhampholeon* (Chamaeleonidae): the role of vicariance and climate change in speciation. Proc R Soc B 271:1967–1975.

McKechnie AE, Wolf BO. 2004. The allometry of avian basal metabolic rate: Good predictions need good data. Physiol Biochem Zool 77:502–521.

McMahon T. 1973. Size and shape in biology. Science 179: 1201–1204.

McMahon TA, Bonner JT. 1983. On Size and Life. New York, NY: W. H. Freeman and Company.

Meyers JJ, Herrel A, Birch J. 2002. Scaling of morphology, bite force, and feeding kinematics in an iguanian and a scleroglossan lizard. In: Aerts P, D'aout K, Herrel A, Van Damme R, editors. Topics in Functional and Ecological Vertebrate Morphology. Maastrict: Shaker Publishing. pp 47–62.

Müller UK, Kranenbarg S. 2004. Power at the tip of the tongue. Science 304:217–219.

Nagy KA, Girard IA, Brown TK. 1999. Energetics of free-ranging mammals, reptiles, and birds. Annu Rev Nutr 19:247–277.

O'Reilly JC. 1998. The scaling of prey capture movements in the Anura [Dissertation]. Flagstaff (AZ): Northern Arizona University. 82 p; Available from: University Microfilms, Ann Arbor, MI; 9918749.

Pennycuick CJ. 1992. Newton Rules Biology: A Physical Approach to Biological Problems. Oxford: Oxford University Press.

Pizzatto L, Almeida-Santos SM, Shine R. 2007. Life-history adaptations to arboreality in snakes. Ecology 88:359–366.

Raxworthy CJ, Forstner MRJ, Nussbaum RA. 2002. Chameleon radiation by oceanic dispersal. Nature 415:784–787.

Richard BA, Wainwright PK. 1995. Scaling the feeding mechanism of largemouth bass (*Micropterus salmoides*): Kinematics of prey capture. J Exp Biol 198:419–433.

Robinson MP, Motta PJ. 2002. Patterns of growth and the effects of scale on the feeding kinematics of the nurse shark (*Ginglymostoma cirratum*). J Zool, Lond 256:449–462.

Roos G, Van Wassenbergh S, Herrel A, Adriaens D, Aerts P. 2010. Snout allometry in seahorses: Insights on optimisation of pivot feeding performance during ontogeny. J Exp Biol 213:2184–2193.

Schwenk K. 2000. Feeding in Lepidosaurs. In: Schwenk K, editor. Feeding: Form, Function, and Evolution in Tetrapod Vertebrates. San Diego: Academic Press. pp 175–291.

Templeton JR. 1970. Reptiles. In: Whittow GC, editor. Comparative Physiology of Thermoregulation, Vol. 1. New York: Academic Press. pp 167–221.

Tilbury CR, Tolley KA. 2009a. A re-appraisal of the systematics of the African genus *Chamaeleo* (Reptilia: Chamaeleonidae). Zootaxa 2079:57–68.

Tilbury CR, Tolley KA. 2009b. A new species of dwarf chameleon (Sauria: Chamaeleonidae, *Bradypodion* Fitzinger) from KwaZulu Natal South Africa with notes on recent climatic shifts and their influence on speciation in the genus. Zootaxa 2226:43–57.

Tilbury CR, Tolley KA, Branch WR. 2006. A review of the systematics of the genus *Bradypodion* (Sauria: Chamaeleonidae), with the description of two new genera. Zootaxa 1363:23–38.

Toro E, Herrel A, Vanhooydonck B, Irschick DJ. 2003. A biomechanical analysis of intra- and interspecific scaling of jumping biomechanics and morphology in Caribbean *Anolis* lizards. J Exp Biol 206:2641–2652.

Townsend T, Larson A. 2002. Molecular phylogenetics and mitochondrial genomic evolution in the Chamaeleonidae (Reptilia, Squamata). Mol Phylogenet Evol 23:22–36.

Townsend TM, Tolley KA, Glaw F, Böhme W, Vences M. 2011. Eastward from Africa: Palaeocurrent-mediated chameleon dispersal to the Seychelles islands. Biol Lett 7:225–228.

Townsend TM, Vieites DR, Glaw F, Vences M. 2009. Testing species-level diversification hypotheses in Madagascar: The case of microendemic *Brookesia* leaf chameleons. Syst Biol 58:1–16.

van Leeuwen JL. 1997. Why the chameleon has spiral-shaped muscle fibres in its tongue. Phil Trans R Soc Lond B 352: 573–589.

Wainwright PC, Bennett AF. 1992. The mechanism of tongue projection in chameleons. II. Role of shape change in a muscular hydrostat. J Exp Biol 168:23–40.

Whitford WG. 1973. The effects of temperature on respiration in the Amphibia. Am Zool 13:505–512.

Wilson RS, Franklin CE, James RS. 2000. Allometric scaling relationships of jumping performance in the striped march frog *Limnodynastes peronii*. J Exp Biol 203:1937–1946.

Zari TA. 1993. Effects of body mass and temperature on standard metabolic rate of the desert chameleon *Chamaeleo calyptratus*. J Arid Environ 24:75–80.